#### RESEARCH ARTICLE



# On the organization of receptive fields of retinal spot detectors projecting to the fish tectum: Analogies with the local edge detectors in frogs and mammals

Elena M. Maximova<sup>1</sup> | Alexey T. Aliper<sup>1</sup> | Ilija Damjanović<sup>1</sup> | Alisa A. Zaichikova<sup>1,2</sup> | Paul V. Maximov<sup>1</sup>

#### Correspondence

Ilija Damjanović, Institute for Information Transmission Problems, the Russian Academy of Sciences, Bolshoy Karetny per. 19, Build. 1, 127051 Moscow, Russian Federation. Email: damjanov@iitp.ru

#### Peer Review

The peer review history for this article is available at https://publons.com/publon/10. 1002/cne.24824.

#### **Abstract**

Responses of ON- and OFF-ganglion cells (GCs) were recorded extracellularly from their axon terminals in the medial sublamina of tectal retino-recipient layer of immobilized cyprinid fish (goldfish and carp). These units were recorded deeper than direction selective (DS) ones and at the same depth where responses of orientation selective (OS) GCs were recorded. Prominent responses of these units are evoked by small contrast spots flickering within or moving across their visual field. They are not selective either to the direction of motion or to the orientation of stimuli and are not characterized by any spontaneous spike activity. We refer to these fish GCs as spot detectors (SDs) by analogy with the frog SD. Receptive fields (RFs) of SDs are organized concentrically: the excitatory center (about 4.5°) is surrounded by opponent periphery. Study of interactions in the RF has shown that inhibitory influences are generated already inside the central RF area. This fact suggests that RFs of SDs cannot be defined as homogeneous sensory zone driven by a linear mechanism of response generation. Physiological properties of fish SDs are compared with the properties of frog SDs and analogous mammalian retinal GCs-local edge detectors (LEDs). The potential role of the SDs in visually guided fish behavior is discussed.

#### **KEYWORDS**

extracellular recording, fish, ganglion cells, retina, retinotectal projections, spot detectors, tectum opticum

#### 1 | INTRODUCTION

The behavior of most fish is largely determined by vision. Cyprinids are characterized by relatively large eyes and complex structure of the retina. There are three types of cones, rods, 12 types of bipolar cells (Li, Tsujimura, Kawamura, & Dowling, 2012), four independent syncytia of horizontal cells (Maximova, 1969; Mitarai, 1982; Stell, Kretz, & Lightfoot, 1982), seven dozen types of amacrine cells (Marc, 1998). These elements being associated in different circuits provide comprehensive processing of the visual scene formed by eye optic on the receptor raster. This can be inferred from the variety of image

properties, detected and transmitted to the brain centers by the output retinal neurons—ganglion cells (GCs) of different types.

The tectum opticum (TO) is the principal visual center in lower vertebrates (fish, amphibians, reptiles) that plays a crucial role in the information processing and control of visually guided behavior. Oculomotor function, used in different modes of behavior, has been maintained in TO throughout the process evolution (Kardamakis, Saitoh, & Grillner, 2015). The fish TO receives 98% of axons of retinal GCs (Northmore, 2011). Axons of various types of GCs terminate at different sublaminae of stratum fibrosum et griseum superficiale (SFGS) in a retinotopic order. Such structure of easily accessible TO

<sup>&</sup>lt;sup>1</sup>Institute for Information Transmission Problems, Russian Academy of Sciences, Moscow, Russian Federation

<sup>&</sup>lt;sup>2</sup>Lomonosov Moscow State University, Faculty of Biology, Moscow, Russian Federation

enables us to study responses of separate retinal GCs by means of extracellular recordings from their axon terminals there. Experiments of this kind can be successfully performed on live animals with intact eye optics, with a set of various visual stimuli. This method not only allows us to study physiological properties of GCs, but also to get closer to understanding their role in the organization of visually guided behavior. The start of this research program was initiated by the article in which the authors directly raised the guestion: "What the frog's eye tells the frog's brain?" (Lettvin, Maturana, McCulloch, & Pitts, 1959). The authors thoroughly investigated physiological properties of GCs projecting to TO of Rana pipiens using their original method. It was shown that: "The retina in the frog is not to transmit information about the point-to-point pattern of distribution of light and dark in the image formed on it. Its function is mainly to analyze this image at every point in terms of four qualitative contexts (standing edges, curvatures, changing contrasts, and local lessening of light intensity) and a measure of illumination and to send this information to the colliculi." Analogical experiments were performed on Rana ridibunda and Rana temporaria and similar types of GCs projecting to TO were revealed (Pigarev & Zenkin, 1970; Vinogradova, Bastakov, Dyachkova, & Manteifel, 1973). Possible role of the described retinal detectors in the organization of frog visually guided behavior was evaluated (for example, spot detector [SD] releases [initiates] hunting behavior while dimming detector—escape and avoidance behavior).

The method applied initially in amphibians was successfully used later in investigations of visual information processing in the fish retinotectal system. The experiments were performed on the live fish with normal blood circulation and intact optics. New types of retinal detectors, formerly not found in frogs, have been described in various fish species such as pike (Zenkin & Pigarev. 1969), trout (Liege & Galand. 1971), several seawater species (Maximova, Orlov, & Dimentman, 1971) and different cyprinids: crucian carp (Maximova & Maximov, 1981), goldfish (Cronly-Dillon, 1964; Jacobson & Gaze, 1964; Maximov, Maximova, Damianović, & Maximov, 2013; Maximov, Maximova, & Maximov, 2005a, 2005b; Wartzok & Marks, 1973), and Japanese dace (Kawasaki & Aoki, 1983). First of all attention was focused on direction selective (DS) GCs. These retinal DS neurons characterized as "fast" DS units are divided into three distinct groups according to their preferred directions of stimulus movement-caudo-rostral, dorsoventral and ventro-dorsal, each group containing DS GCs of ON and OFF subtypes approximately in equal proportion (Damjanović et al., 2019; Maximov et al., 2005a, 2005b). Unlike fish retinae, mammalian retinae (rabbit, mouse, hamster) contain four ON-OFF fast DS GCs each preferring temporo-nasal, naso-temporal, dorso-ventral and ventro-dorsal directions (Barlow & Levick, 1965; Vaney, 1994; Weng, Sun, & He, 2005).

Three principal sublaminae of retinotectal projections in fish TO can be distinguished (Figure 1) (Aliper et al., 2019). Responses of DS GCs are regularly recorded in the superficial sublaminae of the tectal retinorecipient layer. Deeper then DS units at the depth around  $100~\mu m$  the responses of diverse properties are recorded. Among them the most pronounced and easily recognizable are responses of orientation-selective (OS) GCs. They are represented by two types,

one preferring horizontal, another—vertical orientation of the stimulus. Both are indifferent to the sign of the contrast of stimulus, that is, they are ON-OFF type units. They mark this sublaminae (Damjanović, Maximova, & Maximov, 2009b; Maximov, 2010; Maximov et al., 2013; Maximova & Maximov, 1981). And finally, when the electrode is guided deeper than the OS units, sustained activity of another two types of GCs are regularly recorded. The activity of OFF-sustained units is increased by the darkening, whereas the activity of ON-sustained units is intensified by the increased illumination (Aliper, 2018: Maximova et al., 1971).

The responses from a different group of GC units are recorded approximately at the same level of the retinorecipient layer where the OS units are detected, though far less frequently (Aliper et al., 2019). These units are not selective either to the direction of motion or to the orientation of stimuli and are not characterized by any spontaneous spike activity (Aliper et al., 2019; Maximov et al., 2005a; Maximova, Maximov, Damjanović, Aliper, & Zaichikova, 2018). Neither do they respond to the switching of ambient light on and off as well. Prominent response of these units may be evoked by small contrast spot that stands, flickers or moves in their receptive field (RF). Responses of these units to moving small spots are more pronounced than those to moving extended edges or stripes. We refer to these fish GCs as SDs by analogy with the frog SD (Lettvin et al., 1959).

Physiological properties of fish SDs were analyzed and compared with the properties of the frog SDs and analogous mammalian retinal neurons (local edge detectors—LEDs). The potential role of SDs in visually guided behavior is discussed.

#### 2 | MATERIALS AND METHODS

#### 2.1 | Animals

The data were collected from two cyprinid species: *Carassius gibelio*, a wild form of the goldfish and carp (*Cyprinus carpio*). Body weight of the experimental fish varied from 40 g to 100 g. The fish were acquired from local suppliers (Moscow region) and kept in aerated fresh water aquaria at room temperature and natural daylight regime. The fish were treated in accordance with the European Communities Council Directive of 24 November, 1986. The experimental procedures were approved by the local ethical committee of the Institute for Information Transmission Problems of the Russian Academy of Sciences (Protocol No. 1 of April 24, 2018).

#### 2.2 | Preparation

During the experiments the animals were immobilized (d-tubocurarine, i.m.). The dosage of tubocurarine (0.3 mg/100 g of body weight) was adjusted so as to induce the arrest of eyes and respiratory movements. The fish were placed in their natural position in a transparent plexiglas tank where artificial respiration was provided continuously by forcing aerated water through the gills. An opening in the skull was

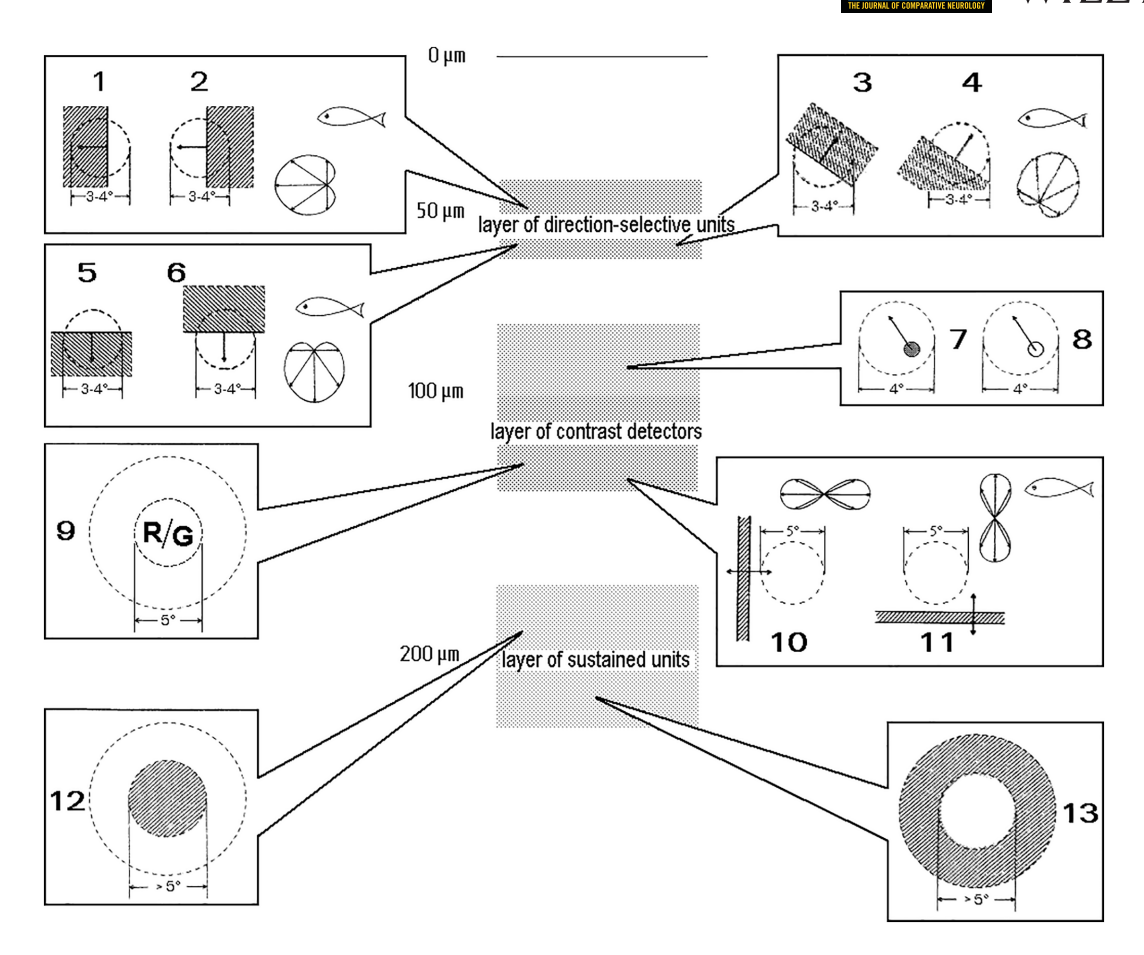


FIGURE 1 Schematic representation of the relative position of various retino-tectal projections in the retino-recipient layer (stratum fibrosum et griseum superficiale [SFGS]) as derived from the extracellular recordings in the goldfish tectum opticum. The thickness of the SFGS is approximately 150  $\mu$ m (from 50 to 200  $\mu$ m of the tectal depth). In the centre, the three sublayers of SFGS are shaded. The detector units of various types recorded at a given depth (indicated in microns) are presented in the frames. These are characterized by the size and shape of the receptive fields (RF), adequate stimulus and polar plot pattern of responses. Superficial sublayer (the depth of about 50  $\mu$ m): 1—ON DS caudo-rostral unit, responding when a dark edge moves out of its RF (circle area of 3–4°) in the caudo-rostral direction (indicated by an arrow); 2—OFF caudo-rostral DS unit, responding when a dark edge moves into the RF; in the bottom right corner of the frame—A polar plot for the caudo-rostral units is shown. In two other frames ON and OFF units of ventro-dorsal (3 and 4) and dorso-ventral (5 and 6) preferred directions are presented. Other conventions are the same as in 1 and 2. Medial sublayer (the depth of about 100  $\mu$ m): detectors of black and white spots (7, 8), rarely recorded color-coding GCs (9), detectors of horizontal (11) and vertical (10) lines are shown. Adequate stimuli — vertical (10) and horizontal (11) stripes are presented near the corresponding eight-shape plots. The deepest sublayer (the depth of about 200  $\mu$ m): Two types of sustained units are shown - those activated by the darkening (12) and the others activated by the lightening (13) of their RFs

made over the midbrain that was contra-lateral to the stimulated eye. Before the surgery the preparation site of the skull was anesthetized with a piece of ice. The borders of the skull opening were moistened with lidocaine. Fatty tissues and cerebrospinal fluid were aspirated and dura mater and pia mater were dissected. The water level in the experimental tank was kept constant, the fish eyes being under the water. The experiment lasted about 8 h, and afterwards the animals were decapitated.

#### 2.3 | Visual stimulation

Computer generated visual stimuli (contrast edges or spots against the background) were presented on the computer-controlled CRT monitor to the fish right eye through the transparent tank wall. Experiments were conducted in the dark room. Distance between the 17 in. monitor screen and the fish eye during the experiments was about 30 cm. At this distance the whole monitor screen occupied  $43^{\circ} \times 32^{\circ}$  of the fish visual field. Stimuli were presented in the limited area of the screen—a square of approximately  $11^{\circ}$  in angular values. The stimulation area could be placed at arbitrary locations of the screen and was usually placed so that the RF of the recorded unit was located approximately in its center. Usually, the luminance of the gray background was maintained at 8.5 cd m<sup>-2</sup>, when expressed in terms of photopic human vision. According to our data (Maximov, Maximova, & Maximov, 2007), the photopic spectral sensitivity of the fish movement detectors (DS GCs, orientation selective GCs, SDs) is determined mainly by its red-sensitive cones. So, it is natural to specify the brightness of the screen "from the point of view" of the red-sensitive cones. In these terms, the background usually has the

effective radiance of 14.5 mW m $^{-2}$  sr $^{-1}$ , and the effective radiances of the light and dark stimuli were 65 and 0.13 mW m $^{-2}$  sr $^{-1}$ , respectively. Constant brightness was maintained for the rest of the monitor screen outside the stimulation area, which effective radiance was usually equal to 7.0 mW m $^{-2}$  sr $^{-1}$ .

#### 2.4 | Recordings and data acquisition

Visual responses are recorded from a contralateral (left) lobe of the TO. Low impedance (200-500  $K\Omega$ ) extracellular microelectrodes made from glass micropipettes filled with the Wood's metal and tipped with a gelatinized platinum cap of 3-5 µm in diameter were used (Gesteland, Howland, Lettvin, & Pitts, 1959). The microelectrode was guided to a required tectal area under a microscope (Olympus SZ51) by means of a micromanipulator (MP-225, Sutter Instrument) according to the retinotopic projection (Jacobson & Gaze, 1964). When the microelectrode is perpendicularly advanced through TO the following general pattern is observed: initial contact with the liquid covering the TO is characterized by an abrupt decrease of background noise, while the subsequent advance of the tip into the superficial TO layers results in noise increase of up to 50 uV and here the first weak neuronal activity can be recorded. The electrode is then carefully advanced through the tectal retinorecipient layer and here the stable single-unit responses of various units may be recorded. Spikes generated from the unit located near the electrode tip are significantly higher in amplitude than those generated by distant sources. Spike amplitudes of single-unit responses usually exceeded the noise amplitude several times and ranged from 200 to 500 µV. Recorded responses are monitored on the oscilloscope and simultaneously listened to on the loudspeaker. In order to select a single unit response, we used amplitude discrimination. Only spikes exceeding the amplitude criterion were used for further analysis. Experimental setup, used for the amplifying, digitizing, storing and processing of the recordings, containing AC preamplifier (band pass 100-3.5 kHz), A/D converter (25 kHz sampling rate) and a system of three mutually connected and synchronized computer modules is described in detail elsewhere (Maximov et al., 2005b; Maximov & Maximov, 2010).

Extracellular responses of retinal GCs axonal endings in TO differ from those of tectal neurons by the waveform of spike and pattern of the discharge. Spikes arriving from the retina usually have triphasic waveform with a negative deflection before the main positive wave. Unlike arriving spikes, spikes generated by tectal neurons and recorded in the vicinity of their cell bodies are biphasic and without initial negative deflection. This difference was already discussed by Lettvin et al. (1959) and Wartzok and Marks (1973). Spikes in the discharge of retinal GCs are equal in amplitude (±noise), whereas the amplitude of the spikes generated by tectal neurons decreases substantially as spike rate increases (Maximov et al., 2005b; Maximova, Pushchin, Maximov, & Maximov, 2012). RFs of putative retinal and tectal units differ dramatically, amounting to 4.5° and 60°, respectively (Damjanović et al., 2009b; Damjanović, Maximova, & Maximov, 2009a; Maximov et al., 2005b). We checked the validity of all

mentioned criteria in the experiments with the application of cobalt chloride solution on the tectal surface to block synaptic transmission between retinal inputs and their targets-tectal neurons. The experimental results supported our considerations: when responses of the putative retinal inputs and the supposed tectal neurons were simultaneously recorded with the same microelectrode position, the application of solution of cobalt chloride resulted in degradation and disappearance of the response of putative tectal neurons, while responses of retinal axon terminals remained intact. The effect of the blockade may be washed by physiological Ringer solution and restored by new application of cobalt chloride (Maximova et al., 2012). The data consistent with our findings have been demonstrated in zebrafish juveniles by means of Ca++ imaging method (Abbas, Triplett, Goodhill, & Meyer, 2017; Nikolaou et al., 2012). Axon terminals of three types of DS GCs that prefer three directions and two types of OS GCs were detected in the tectal retinorecipient layer. The stratification of these axon terminals coincides with the stratification of retinotectal projections described in our studies.

#### 2.5 | Experimental procedures

The standard experimental procedures (generation of polar diagrams, random checkerboard etc.) were designed in the form of a series of program tools.

The polar diagram (PD)-the visualization of the dependence of the strength of response (number of spikes) on the direction of stimulus movement was measured for each of recorded units in order to determine its type (DS, orientation selective or nonselective) (Maximov et al., 2005a). Some of recorded nonselective units did not respond to the edge stimulus (wide stripe exceeding stimulation area in width). In those cases, PDs were measured with moving contrast spots. The stimuli moved across the stimulation area in 12 or 24 different directions in a random order (three runs in each direction). An additional stimulus run was performed in the initial (first) direction in order to check for the unit's response stability. The position of the unit's RF was specified using experimental data obtained during the polar diagram measurements. The RF center was evaluated from the sequences of moments of spike appearances in all trials for all directions of movement, by the custom-made program tools described elsewhere (Damjanović et al., 2009a).

RFs of the recorded units were mapped by the canonical method with a flickering contrast spot ("random checkerboard"). The area of stimulation was divided into 49 small squares (spots) with sides slightly exceeding 1°. The stimuli were flashed on and off sequentially in a quasi-random order (the stimuli were presented three times at each position). The number of spikes evoked by each sequential turning the spot on and off was counted. Stimulation was always initiated in the central spot. At the end of the procedure, stimulation was repeated at the central position in order to check for the unit's response level. The estimated position and shape of the RF were evaluated by the use of the following procedure. The responses of the unit (numbers of spikes) to flashing spots were considered as random

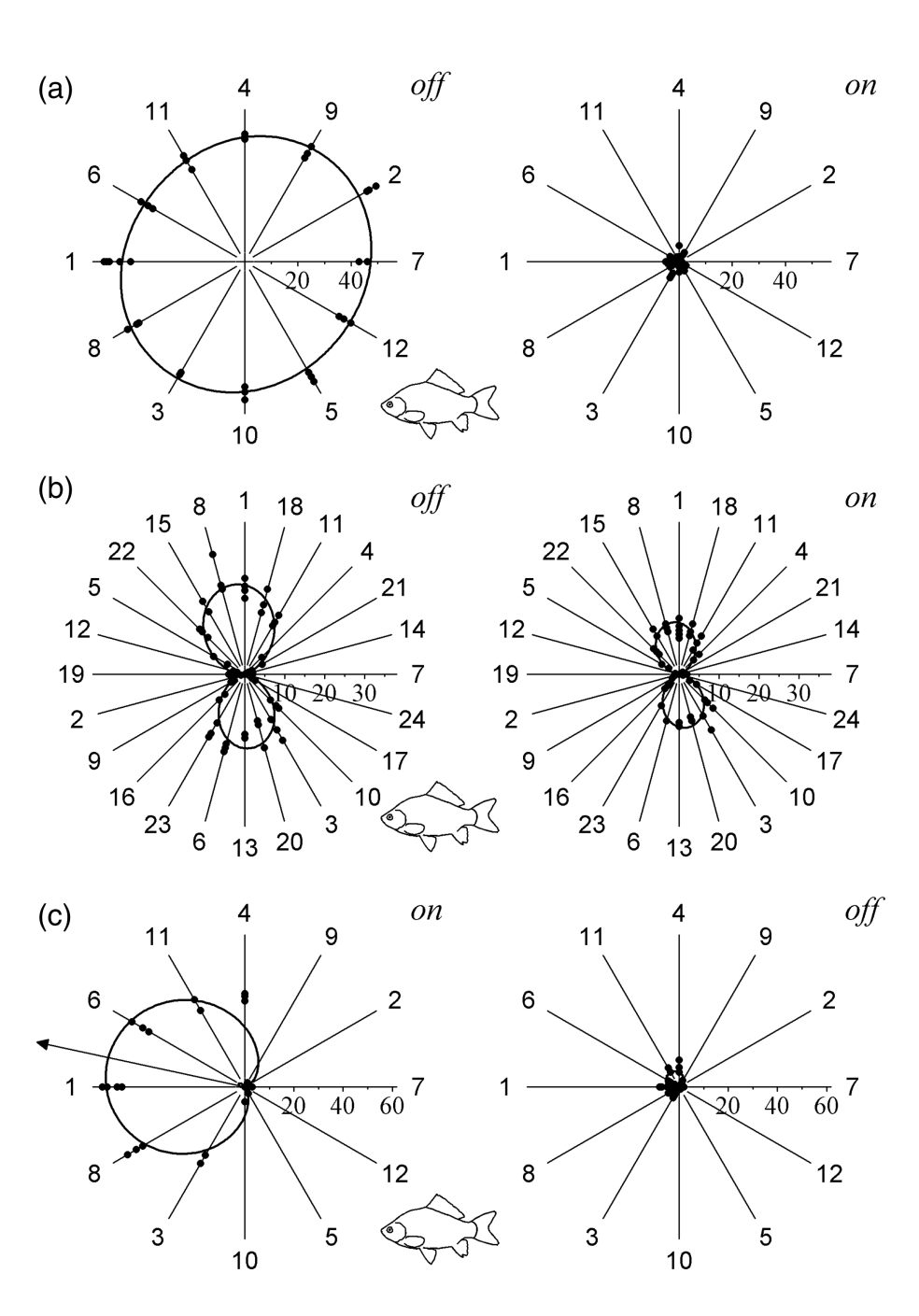
values distributed normally along the stimulation area, and the parameters of this two-dimensional normal distribution (mean values, variances and correlation coefficient) were calculated. Then the probability density function z = f(x, y) was built with the maximum value  $f_{\text{max}} = f(x_0, y_0)$  at the estimated center of the RF. After that this function was intersected by the plane  $z = f_{\text{max}}/e$ , and the resulting ellipse was interpreted as an estimated border of the unit's RF (Damjanović et al., 2009a).

Lateral interactions in the RFs of the recorded units were analyzed by the test which consisted of stimulation by concentric spots of different sizes. Flickering spots of different widths were presented in the RF center sequentially in quasi-random order (three times for each width). The relationship between the cell response (number of

spikes) and the width of the stimulus was analyzed. This procedure will be hereinafter referred to as "RF width" (RW).

Dependence of SDs response on the stimulus intensity was investigated by means of separate experimental procedure. This procedure, designed in a form of program tool, was as follows. Stimuli were contrast edges or spots of different brightness. Edges of different brightness moved (three times each) over neutral gray background, and number of spikes evoked by leading and trailing edges of stimuli were counted. Sometimes we used stationary spots of different brightness flickering in the center of the RF instead of contrast edges and responses to onset and offset of stimuli were counted. Graphs, representing dependence of the mean number of spikes on the brightness of stimuli, were constructed (see Figure 4,

**FIGURE 2** Polar plot of a black spot detector (BSD) as compared with polar plots of direction selective and orientation selective units. Stimuli (contrast edges) moved in 12 (a and c) or 24 (b) directions at the speed of 11°/s inside the gray stimulation area (a square with a side of approximately 11° on the monitor screen). Polar plots of responses to the leading (left panel) and trailing (right panel) edges of stimuli are shown. Dots mark the number of spikes evoked in response to each of three runs for each applied direction (numbers in scales represent number of spikes in responses); solid curves represent the approximations of the experimental data by a Fourier series with first two harmonics. Numbers on the radial lines represent the order of movement direction. The plots marked with the label "off" are built for the responses to the movement of dark edges into the receptive field (RF), those marked with label "on" are built for the responses to the movement of light edges. Orientation of the fish relative to directions of stimulus movement is demonstrated. (a) BSD: stimulus-black edge; (b) detector of horizontal line (ON-OFF unit); stimulus-black edge; (c) ON-DS caudo-rostral unit; stimulus-White edge; preferred direction of stimulus' movement for the unit is shown by the black arrow. Edge stimulus-wide stripe exceeding stimulation area in width



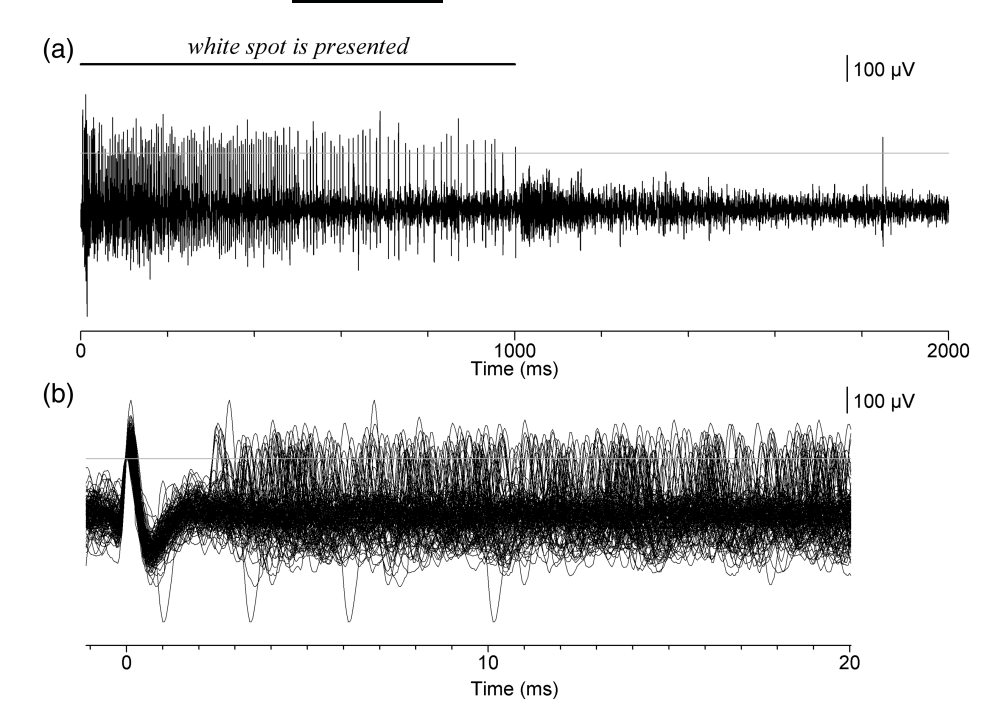
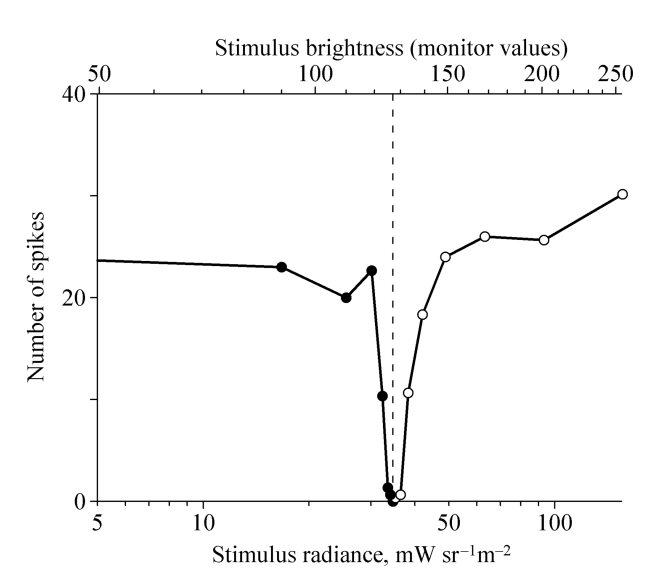


FIGURE 3 The response of a white spot detector (WSD). (a) The response of a WSD to the small stationary white spot that flashed in the center of the unit receptive field (RF) against a neutral (gray) background. Spot diameter-1.1°; duration of the stimulation-1 s (marked by the horizontal bar at the top panel of the figure). Thin horizontal line represents a criterion level (220  $\mu$ V) used for amplitude discrimination of spikes. Only spikes exceeding the amplitude criterion were used for further analysis. (b) Superimposed individual spikes from the WSD train, synchronized by each spike that has passed the threshold of discrimination, shown in the extended sweep. Absence of spikes in the refractory period indicates that the spikes filtered by the amplitude criterion belong to the single unit



**FIGURE 4** Intensity–response profiles showing the responses of simultaneously recorded white spot detector (WSD) and black spot detector (BSD) as functions of the light intensity. The ordinate indicates the number of spikes (mean of three runs) in units' discharges in response to the onset of achromatic spots of various intensities flashing (flickering) over a fixed gray background. White circles indicate WSD responses, black ones—BSD responses. Saturation of profiles at low contrast stimuli suggests that responses of both recorded units are practically independent of the stimulus intensity. The background radiance was equal to 34.6 mW sr<sup>-1</sup> m<sup>-2</sup> (marked with dashed line). The diameter of flashing spot was 41 pixels, or 2.2°. Weber contrast thresholds for the WSD and the BSD are 4.0 and –2.5%, correspondingly

representing data for two simultaneously recorded SDs). This experimental test will be hereinafter referred to as "Black and White" procedure ("BW").

#### 3 | RESULTS

#### 3.1 | General properties of the fish retinal SDs

The segregation of different retino-tectal projections, revealed by means of extracellular recordings in the fish tectum (Maximova et al., 1971; Maximov et al., 2005a, 2005b; Aliper et al., 2019), is consistent with the pattern demonstrated by classical morphological methods (Meek & Schellart, 1978), as well as with the new methods of Ca++ imaging and Brainbow genetic labeling (Abbas et al., 2017; Nikolaou et al., 2012; Robles, Filosa, & Baier, 2013; Robles, Smith, & Baier, 2011). Units with different properties are sequentially recorded in different TO layers during the perpendicular advance of a microelectrode. Single-unit responses of various types occur in the following order. Retinal DS units are located at the depth of about 50 μm. Retinal orientation selective units are located in the underneath sublaminae, at the depth of about 100 µm. And finally, sustained responses of two other ON- and OFF-types of GCs are recorded at the depth of about 200 µm, deeper than all other retinal units (Aliper et al., 2019).

As mentioned above, the responses from SDs are recorded approximately at the same level of the retinorecipient layer where the OS units are detected, though far less frequently. Polar diagrams were measured in 233 SDs. Second-order harmonic function was used to approximate experimental data:

$$N(\varphi) = a_0 + a_1 \cos(\varphi - \varphi_1) + a_2 \cdot \cos(\varphi - \varphi_2)$$

The amplitudes of the zero  $(a_0)$ , first  $(a_1)$ , and second  $(a_2)$  harmonics, and the phases of the first  $(\varphi_1)$  and second  $(\varphi_2)$  harmonics characterize the polar response patterns. Polar plots of recorded SDs did not substantially differ from each other. They were characterized

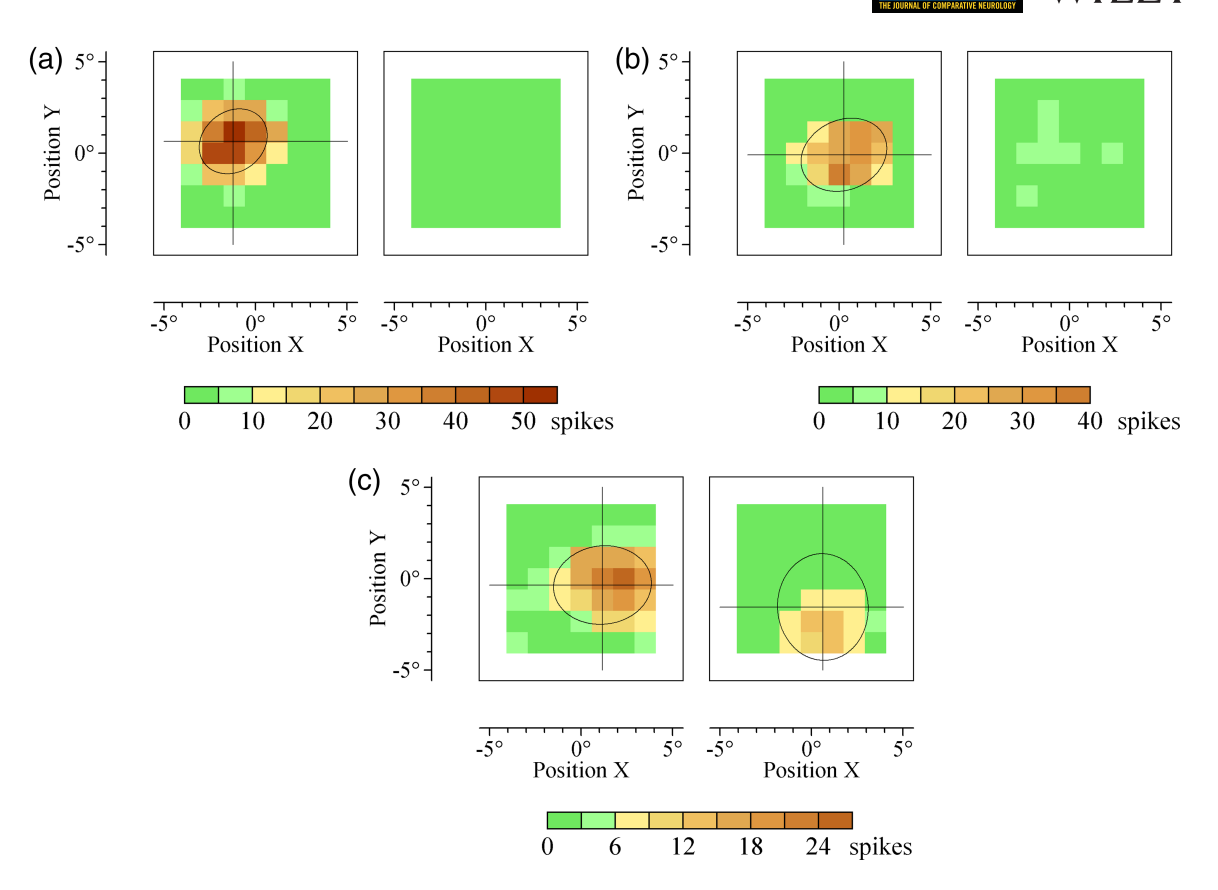
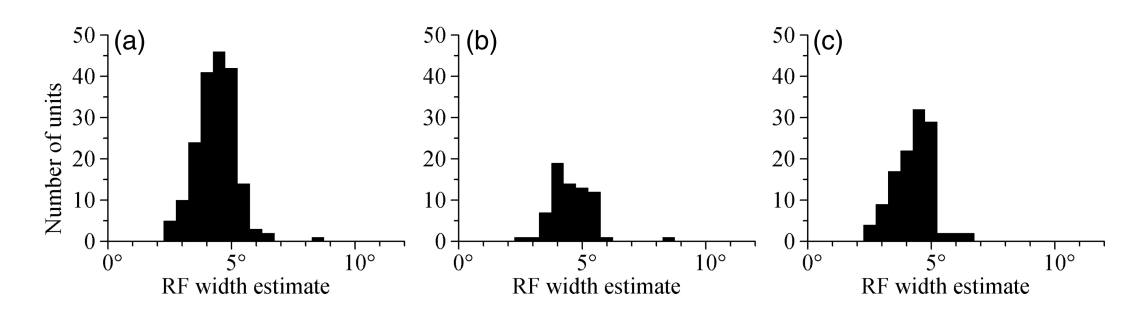


FIGURE 5 Maps of receptive fields (RFs) of different spot detectors (SDs), measured by canonical random checkerboard method. (a) RF map of a white spot detector (WSD) (single unit recording). Stimulus—a white spot flashing on and off across the gray background. There is no response to the offset of stimulus. (b) RF map of a black spot detector (BSD) (single unit recording). Stimulus—A black spot flashing on and off across gray background. There is no response to the offset of stimulus. (c) RFs of two neighboring SDs WSD and BSD ("paired recording") mapped with white spot switched on and off across gray background. There are responses to the onset and offset of the stimulus. RF maps on the right and left panels are slightly shifted relative to each other, which points to a "paired recording". On the left panels—unit responses to the onset of stimuli; on the right panels—unit responses to the offset of stimuli. The area of stimulation—a square with a side of approximately 11°, stimulus—the spot was a square with a side of approximately 1.1° flashed on and off sequentially in different positions of the square grid in a quasi-random order three times at each position, duration of stimulus was 1 s. Number of spikes was counted after each turning on and off of the spot. Unit responses over the entire stimulation area, measured by this method, are represented in the form of a topographic map (see the scale at the bottom). Units' RFs are indicated by ellipses [Color figure can be viewed at wileyonlinelibrary.com]



**FIGURE 6** Receptive fields (RFs) sizes of spot detectors (SDs) measured by random checkerboard method. (a) Histogram of distribution of the RF sizes, calculated for 188 SDs (among them 69 WSDs and 119 BSDs). (b) Distribution of the RF sizes, calculated separately for WSDs. (c) Distribution of the RF sizes, calculated separately for BSDs. The average size of the RF for all recorded units:  $4.6 \pm 0.8^{\circ}$  (WSDs =  $4.8 \pm 0.8^{\circ}$ ; BSDs =  $4.5 \pm 0.8^{\circ}$ ) (standard deviation: 1-sigma)

by relatively small amplitudes of both, first and second harmonics. Typical polar plot of a SD is presented in Figure 2a. Polar plots of an OS and a DS unit are shown in Figures 2b,c for comparison. It is clearly seen that fish SDs unlike two other GC types are not selective

either to the direction of motion or to the orientation of stimuli. In previous studies we have clearly shown that according to their polar plot patterns, GCs projecting to the tectum indeed constitute three clear clusters: (a) those with small relative amplitudes of both, first

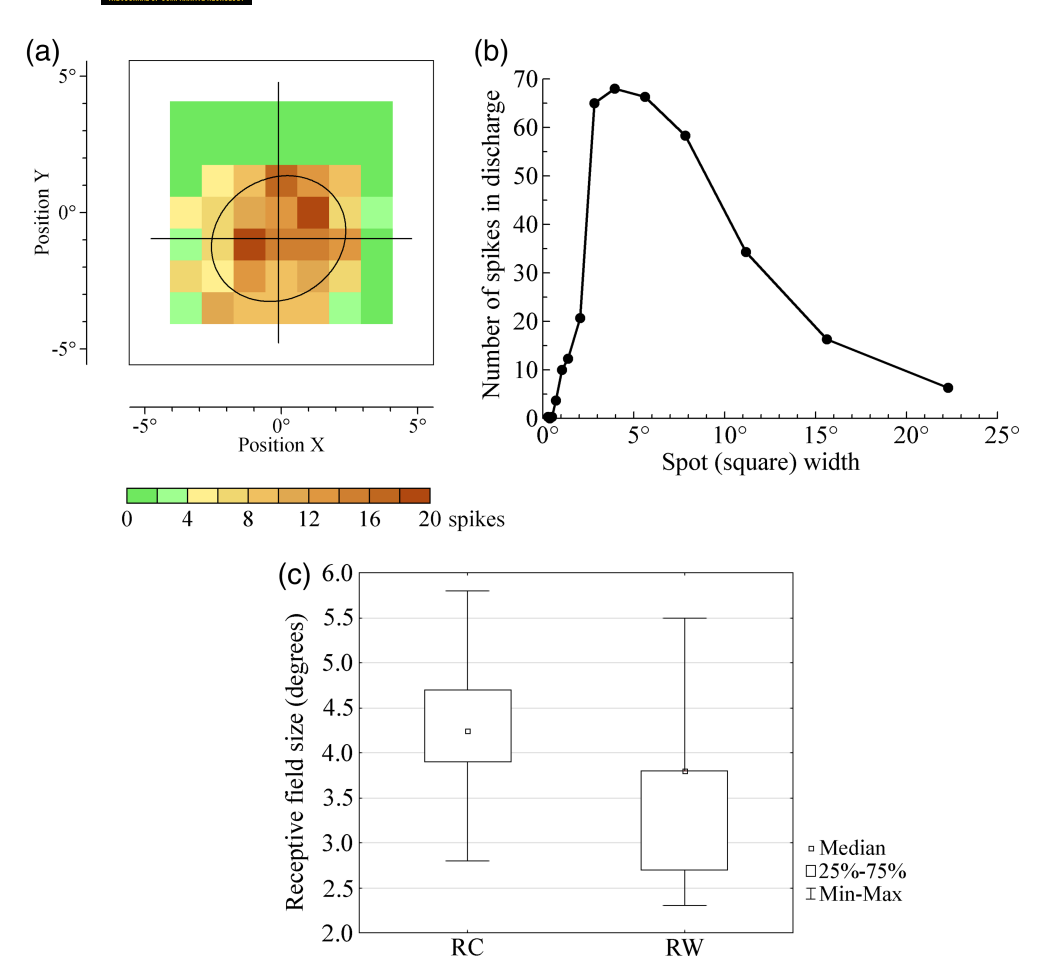


**FIGURE 7** Excitation and inhibition in the receptive field (RF) of a black spot detector. (a) RF of a black spot detector (BSD) mapped by means of the random checkerboard method. Other conventions are the same as in Figure 5. (b) Responses of the same BSD induced by black concentric flashing spots of different sizes ("RW" method). Flickering spots of different widths were presented in the RF center sequentially in quasi-random order. Stimuli were presented three times for each width and averaged responses of the unit were calculated. Abscissa: The stimulus width (degrees); ordinate: Number of spikes in the unit discharge in response to stimulus onset. (c) Statistical analysis of the difference between RF widths of 43 SDs measured by two methods: "Random checkerboard" ("RC") and "RW". Difference between two sets of data is statistically significant at p < .05 (Mann–Whitney U test; p = .00071). Detailed explanation is provided in the text [Color figure can be viewed at wileyonlinelibrary.com]

and second harmonics—nonselective units; (b) those with pronounced relative amplitude of the first harmonic - direction-selective units; (c) those with pronounced relative amplitude of the second harmonic—orientation-selective units (Maximov et al., 2005a, 2005b).

Characteristic feature of these units is prolonged response to small stationary spot, lasting for seconds (Figure 3a). As a rule, spot that flashes in the center of the RF evokes sustained response whereas a stimulus presented a little aside from the RF center evokes transient discharge. The stimulation with flashing spots (white or black against gray background) reveals that there are two types of such units—ON and OFF ones. ON units respond to a white stimulus turning on and to a black one turning off. OFF units, on the contrary, discharge when a black spot turns on or a white spot turns off. These units are referred to as white SDs (WSDs) and black SDs (BSDs), correspondingly. Responses of 332 SDs have been recorded—204 OFF-units and 128 ON-units. The response of a WSD to the onset of the flickering white spot is demonstrated in Figure 3a. In order to select a single unit response, we used amplitude discrimination. Superimposed

individual spikes from the WSD train, synchronized by each spike that has passed the threshold of discrimination are demonstrated in Figure 3b. Absence of spikes in the refractory period indicates that the spikes filtered by the amplitude criterion belong to the single unit.

Sometimes flickering spot simultaneously evokes both ON and OFF responses of practically equal amplitudes. However, in the majority of such cases it was unequivocally proved that we simultaneously recorded from two separate SDs (ON and OFF units), whose RFs were slightly displaced from each other. One can imagine that axon terminals of these units are located near each other on the practically same depth, and their responses may be recorded simultaneously (Figure 5c).

Typical intensity-response profiles of SDs measured by means of "BW" procedure are presented in the Figure 4 (two simultaneously recorded WSD and BSD). The profiles saturate at low contrast stimuli what indicates that SDs work practically according to the "all-or-non" law similar to DS GCs and OS GCs (Maximov, 2010; Maximov et al., 2005b).

#### 3.2 | Receptive fields

RFs of the recorded units were mapped by the canonical method with a flickering contrast spot ("random checkerboard"). Examples of RF mapping for a WSD and a BSD are shown in Figure 5a,b. The units were excited by adequate stimuli-WSD with the white spot and BSD with the black spot. Stimuli, 1.1° in diameter, flashed on and off sequentially in a quasi-random order over the gray stimulation area. One can see that in both cases only stimulus onset evoked prominent response of the unit. Both units were characterized by relatively small RF areas of about 4° in diameter (see ellipses which represent estimations of units' RFs). However, as mentioned above, sometimes flickering spot simultaneously evokes ON and OFF responses of practically equal amplitudes. In such cases, as a rule, RFs mapped for stimulus onset and offset are slightly shifted relative to each other. This indicates that we record from two separate SDs located in close proximity to each other (Figure 5c). Random checkerboard method was applied to 119 BSDs and 69 WSDs. Distributions of RF sizes, calculated separately for BSDs and WSDs, are shown in Figure 6. Averaged RF diameters of two types of units were almost equal:  $4.8 \pm 0.8$   $^{\circ}$  for WSDs and 4.5  $\pm$  0.8  $^{\circ}$  for BSDs (4.6  $\pm$  0.8  $^{\circ}$  for all recorded units). RF size of 4.5° corresponds to 300 μm approximately (Damjanović et al., 2009a).

Lateral interactions in the RFs of the recorded units were analyzed by the RW test which consisted of stimulation by concentric spots of different sizes. The results of this test applied on a BSD are shown in Figure 7b. One can see that the number of spikes in the unit response initially increases with an increase of the width of the stimulus up to some "optimal size." And then it starts to decrease, which points at the start of lateral inhibitory influences. Inhibition started after the stimulus width of 3.8° (Figure 7b). The width of the central RF excitatory area calculated by the "random checkerboard" method was approximately 4.6° (Figure 7a), what indicates that inhibition starts already near the border inside the RF center.

Hence, we have tried to estimate the size and the structure of the RFs using random checkerboard and RW procedure. However, as stable recording could not be maintained for the period of time long enough to do all measurements, both procedures were successfully performed together only in 43 cells—28 WSDs and 15 BSDs. Averaged RF diameter measured by random checkerboard for all 43 units was  $4.3 \pm 0.7^{\circ}$ . According to the RW test inhibition in the same units started after the averaged stimulus width of  $3.8 \pm 1.0^{\circ}$ . Difference between RF widths measured by two methods was statistically significant (Figure 7c; Mann–Whitney U test). Estimation of the excitatory RF area by "RW" method was significantly lower than that evaluated by random checkerboard, what indicates that inhibition starts already inside the excitatory RF center.

#### 4 | DISCUSSION

#### 4.1 | Physiological properties of SDs

There are two types of retinal units projecting to the fish TO especially sensitive to small contrast spots moving or flickering (flashing) in

their RFs. At the same time, they do not respond to ambient light changes (switching on or off the illuminant). These two types differ from each other only by the preferred sign of stimulus contrast against the background. Both of them are not selective either to the direction of motion or the orientation of prolonged visual stimuli, edges or stripes. The response to a moving spot is always more prominent than responses to contrast stripes or edges. RFs of SDs are characterized by the center-surround organization—the excitatory central area and inhibitory surround. Responses of SDs to stimuli larger than the RF center abruptly decrease because of strong inhibition of the surround (Figure 7a,b). Comparison between sizes of excitatory RF area measured in 43 SDs by two methods, random checkerboard and "RW," showed that two sets of data significantly differ from each other (Figure 7c). Estimation of the excitatory area by "RW" method was significantly lower than that evaluated by random checkerboard, what indicates that the optimal size of the stimulus is smaller than the size of RF central area, that is, inhibitory influences are generated already inside the RF center. This fact suggests that responses to stimuli of different widths are not results of linear spatial summation inside the RF. Absence of linear signal summation across RF indicates that RFs of SDs cannot be defined as homogeneous sensory zone driven by a linear mechanism of response generation. Furthermore, SDs with their RF center of about 4.5° can distinguish moving or stationary spots of 0.16°, the smallest size that we are able to present on the monitor screen. This indicates that spatial visual acuity of SDs is much higher than the acuity provided by the linear RF of the appropriate size. The same phenomenon was observed in DS as well as orientation selective GCs (Maximov et al., 2013).

Physiological features similar to those described in fish SDs characterize frog SDs and mammalian LEDs. Both, frog and mammalian analogs of fish SDs are characterized by relatively small RFs, poorly respond to ambient light changes and are not selective either to the direction of motion or to the orientation of stimuli. (Baden et al., 2016; Lettvin et al., 1959; Manteifel & Bastakov, 1989; van Wyk, Taylor, & Vaney, 2006). However, one substantial difference between the frog, mammalian and the fish SDs should be pointed. The frog SDs are exclusively OFF-type units, mammalian ones ON-OFF type units, while the fish detectors comprise two types—ON and OFF SDs.

There are two principal questions to be answered in the study of GC's properties:

- 1. What is the morphological base that ensures physiological properties of a certain type of GCs?
- 2. What is the role of a given type of GC in the visual processing?

One can expect that similar physiological properties are supported by similar morphology in different animals. There is no information about the fish and frog SDs' morphology because all the physiological data have been collected by extracellular recordings in the TO. On the contrary, detailed information was collected on morphological characteristics of rabbit LEDs and their analogs W3 cells of the mouse retina (Baden et al., 2016; Famiglietti, 2005a, 2005b; Levick, 1967; Sümbül et al., 2014; van Wyk et al., 2006; Zhang, Kim,

Sanes, & Meister, 2012). On the flat preparation of the retina it was clearly seen that the dendritic trees of neighboring LEDs substantially overlap-as a rule the endings of dendrites of one cell almost reach the soma of the neighboring cell (van Wyk et al., 2006). Such dendritic mosaic is not characteristic for the other types of GCs, including DS GCs whose dendritic trees approach one another but do not overlap (i.e., the "dendritic tiling") (Field & Chichilnisky, 2007; Masland, 2012). The inhibitory influences in RFs of the fish SDs and mammalian LEDs are evidently different in their nature from the asymmetric "null-side" inhibition described for the DS GCs (Briggmann, Helmstaedter, & Denk, 2011). On the vertical reconstruction of the rabbit and mouse retinae it is clearly seen that the LED dendritic trees are located in between the two dendritic arborizations of the fast ON-OFF DS GCs (Baden et al., 2016; van Wyk et al., 2006; Zhang et al., 2012). This indicates that the LED dendritic arborizations are located outside of the starburst AC dendritic sublaminae, therefore inhibitory influences within their RFs cannot be mediated by the GABAergic synapses of starburst ACs as it is the case for the DS GCs, but by certain different amacrine cells (possibly by some type of the glycinergic ones). LEDs in the mammalian retina are mainly located in the ON sublayer of the inner plexiform layer but close to the edge between ON and OFF sublaminae, which enables them to receive inputs from both types of bipolar cells (Famiglietti, 2005a, 2005b). Accordingly, the mammalian LEDs belong to the ON-OFF type of GCs, unlike the fish SDs that respond either to light-ON (ON-units) or light-OFF (OFF-units). Irrespective of this difference, similar physiological properties of the two types of units point to the analogy in the structure of their RFs.

Specialized GCs analogous to the rabbit and mouse LEDs were described in other mammals. Lucifer Yellow-stained "zeta cells" of the ferret retina were characterized by one of the smallest dendritic fields among GCs (Wingate, Fitzgibbon, & Thompson, 1992). Cat "zeta cells" which correspond to the transient "W" cells, were also classified as LEDs (Berson, Pu, & Famiglietti, 1998; O'Brien, Isayama, & Berson, 1999). These GCs are very similar to LEDs of the rabbit retina and possibly homologous to the "maze cells" of the macaque retina (Rodieck & Watanabe, 1993).

## 4.2 | "Detector concept" and the new concept of exogenous guidance of visual attention as a universal function of the TO across vertebrates

## 4.2.1 | Experimental facts that support "detector concept"

TO of the lower vertebrates (fish, amphibian), which receives a considerable amount of visual information that has been already partially processed, is involved in the organization of various forms of behavior. It includes hunting (foraging) and defensive behavior, avoidance of obstacles, etc. The correlation of the activity of particular types of GCs with specific forms of behavior was thoroughly studied in experiments on frogs and toads. The first investigators who used the "concept of feature detectors as the key-detectors" in order to relate

activity of a certain GC type (detector) to a specific form of the frog behavior were Barlow (1953) and Lettvin, Maturana, McCulloch, and Pitts (1959). Later on the "detector concept" was confirmed in a number of electrophysiological and behavioral studies. Dependence of the toad behavior on the size of stimulus (black spot) was clearly shown in behavioral experiments: small spots triggered hunting behavior while large stimuli, on the contrary, induced the avoidance response (hiding). The switch from one mode of behavior to the other happened abruptly after the size of the stimulus had reached a certain value (Ewert, 1970). In the study of Pigarev and Zenkin (1970) the activity of SDs was recorded for a freely moving frog. It was shown that the activation of a SD always precedes the snapping of tongue.

In separate experiments the regeneration of different forms of the frog visually guided behavior was followed after the transection of the optic nerve (Vinogradova et al., 1973; Manteifel & Bastakov, 1989). It was shown that different forms of behavior (avoidance of obstacles, foraging) regenerated over different time intervals, along with the optic nerve regeneration and subsequent activation of different types of detectors recorded in the TO. Last of all (200 days after the transection) regenerated the electrical activity of SDs and the foraging behavior. On the basis of all of the abovementioned studies one can conclude that the SDs recorded in the frog (toad) tectum detect the "key stimulus" within the visual scene, which triggers the hunting behavior in the animal.

Recent observations on free-ranging as well as partially restrained zebrafish larvae showed that the fish responded to moving stimuli in a size-dependent manner too. Small moving spots (1°) evoked convergent eye movements and J-turns of the tail in restrained larvae, which are defining features of natural hunting behaviour. Free-ranging fish directed multiple low amplitude orienting turns (~20°) toward small moving spots (1°) and high-amplitude aversive turns (~60°) from larger spots (10°) (Bianco, Kampff, & Engert, 2011). Prey capture is initiated within a narrow range of stimulus size and velocity (Trivedi & Bollmann, 2013). It was shown that moving objects which resemble prey or predator evoke electrical activity in different fibers (axons of different types of GCs) projecting to the zebrafish TO (Preuss, Trivedi, vom Berg-Maurer, Ryu, & Bollmann, 2014). The tectum categorizes visual targets on the basis of retinally computed size information, suggesting a critical role in visually guided response selection. BSDs that we record in the goldfish and the carp TO could be considered as triggers of foraging behavior similar to the ones in the zebrafish and frogs.

## 4.2.2 | Facts that contradict the "detector concept"

In the frame of the "detector concept" it would be logical to expect that in animals living in different natural habitats and demonstrating different types of behavior, different sets of detectors should be presented in the tectum. The data progressively collected over a long period of time call into question the absolute meaningfulness of the "detector concept." So in fish, characterized by the enormous

taxonomic, ecological and ethological diversity, one and the same set of retinal feature detectors was described in the TO of all of the studied species (Cronly-Dillon, 1964; Damjanović, Maximova, Aliper, Maximov, & Maximov, 2015; Jacobson & Gaze, 1964; Liege & Galand, 1971; Maximov et al., 2005a, 1971; Zenkin & Pigarev, 1969). Furthermore, practically the same set of specialized GCs was described in retinae of various mammals (Masland, 2012; O'Brien et al., 1999; van Wyk et al., 2006; Venkataramani & Taylor, 2010). Till the present time more than 20 morphophysiological types of GCs were described in different animals (Masland, 2001; Robles et al., 2013; Volgyi, Chheda, & Bloomfield, 2009). It will not be correct to attribute the functions of the "key-detectors" to each type of retinal GCs. While the properties of many types of specialized GCs—movement detectors (DS GCs, OS GCs) are rather well-investigated, their functions remain obscure.

### 4.2.3 | Contemporary view on the function of retinal movement detectors

In view of the foregoing, the retinal movement detectors (SDs, DS GCs, OS GCs) should be considered as some basic elements of preliminary image processing. Contemporary concept of their function is that they are the "feature detectors" which form a saliency map associated with the motor map in the TO in the lower vertebrates. Basic role of tectum is gaze-control organization, that is, detection of the most important stimulus (pop-out) on the saliency map and also suppression of potential targets of low interest. Recent studies suggest possible cellular circuits (Ben-Tov, Donchin, Ben-Shahar, & Segev, 2015; Kardamakis et al., 2015; Sridharan, Schwarz, & Knudsen, 2014; Zhaoping, 2016). Fish SDs that we describe here are "feature detectors" and at the same time the "key detectors" which trigger prey-catching, that may be concluded from behavioral experiments mentioned above.

In mammals along with the quantitative redistribution of retinal inputs from retino-tectal to retino-geniculo-cortical pathways in the course of the evolutionary process the saliency map had moved from the tectum to the primary visual cortical zone V1 (Zhaoping, 2016). DS and OS GCs were not detected in the primate retina, while the neurons with analogical properties were found in the lateral geniculate body and primary visual cortex (V1) (Hubel & Wiesel, 1968).

The oculomotor—gaze-control function (gaze stabilization on a visual object or gaze shift to another pop-out stimulus), that is, the external guidance of visual attention is preserved at the tectal level across all vertebrates from lamprey to primates, which may be inferred from the striking similarities of the tectal circuitry of the earliest family of vertebrates that diverged from the main vertebrate line as early as roughly 560 million years ago, to that of the more recent vertebrate groups of species (Kardamakis et al., 2015).

#### **ACKNOWLEDGMENTS**

Authors are grateful to Anna Kasparson who provided improvements to our English grammar.

#### **CONFLICT OF INTEREST**

The authors declare no conflicts of interest.

#### **AUTHOR CONTRIBUTION**

All authors had full access to all the data in the study and take responsibility for the integrity of the data and the accuracy of the data analysis. Design of the study: E.M.M., I.D. Design of experiments: E.M.M., A.T.A. Acquisition, analysis and interpretation of data: EMM, P.V.M., I.D., A.A.Z. Preparing the figures: P.V.M., A.A.Z., I.D. Technical support: A.T.A., P.V.M. Drafting of work and critical revision for important content: E.M.M.

#### DATA AVAILABILITY STATEMENT

Data openly available in a public repository that issues datasets with DOIs

#### ORCID

Ilija Damjanović https://orcid.org/0000-0002-8756-3433

#### **ENDNOTE**

<sup>1</sup> However, this is not always the case. For example, GC direction selectivity can be generated on the basis of different morphological pathways in the retina (Kim, Zhang, Yamagata, Meister, & Sanes, 2008).

#### **REFERENCES**

- Abbas, F., Triplett, M. A., Goodhill, G. J., & Meyer, M. P. (2017). A three-layer network model of direction selective circuits in the optic tectum. Frontiers in Neural Circuits, 11, 88.
- Aliper, A. T. (2018). Receptive field sizes of sustained ganglion cells in the goldfish retina. *Sensornye Sistemy*, 32, 8–13 (in Russian).
- Aliper, A. T., Zaichikova, A. A., Damjanović, I., Maximov, P. V., Kasparson, A. A., Gačić, Z., & Maximova, E. M. (2019). Updated functional segregation of retinal ganglion cell projections in the tectum of a cyprinid fish—Further elaboration based on microelectrode recordings. Fish Physiology and Biochemistry, 45, 773–792.
- Baden, T., Berens, P., Franke, K., Roson, M. R., Bethge, M., & Euler, T. (2016). The functional diversity of retinal ganglion cells in mouse. *Nature*, 529, 345–350.
- Barlow, H. B. (1953). Summation and inhibition in the frog's retina. *Journal of Physiology (London)*, 119, 69–88.
- Barlow, H. B., & Levick, W. R. (1965). The mechanism of directionally selective units in the rabbit's retina. *Journal of Physiology (London)*, 178, 477–504.
- Ben-Tov, M., Donchin, O., Ben-Shahar, O., & Segev, R. (2015). Pop-out in visual search of moving targets in the archer fish. *Nature Communications*. 6. 1–11.
- Berson, D. M., Pu, M., & Famiglietti, E. V. (1998). The zeta cell: A new ganglion cell type in cat retina. *Journal of Comparative Neurology*, 399, 269–288.
- Bianco, I. H., Kampff, A. R., & Engert, F. (2011). Prey capture behavior evoked by simple visual stimuli in larval zebrafish. Frontiers in Systems Neuroscience. 5. 10.
- Briggmann, K. L., Helmstaedter, M., & Denk, W. (2011). Wiring specificity in the direction-selectivity circuit of the retina. *Nature*, 471, 183–188.
- Cronly-Dillon, J. R. (1964). Units sensitive to direction of movement in goldfish tectum. *Nature*, 203, 214–215.
- Damjanović, I., Maximova, E. M., Aliper, A. T., Maximov, P. V., & Maximov, V. V. (2015). Opposing motion inhibits responses of direction-selective ganglion cells in the fish retina. *Journal of Integrative Neuroscience*, 14, 53–72.

- Damjanović, I., Maximova, E. M., Aliper, A. T., Zaichikova, A. A., Gačić, Z., & Maximova, E. M. (2019). Putative targets of direction-selective retinal ganglion cells in the tectum opticum of cyprinid fish. *Brain Research*, 1708. 20–26.
- Damjanović, I., Maximova, E. M., & Maximov, V. V. (2009a). Receptive field sizes of direction-selective units in the fish tectum. *Journal of Integra*tive Neuroscience, 8, 77–93.
- Damjanović, I., Maximova, E. M., & Maximov, V. V. (2009b). On the organization of receptive fields of orientation-selective units recorded in the fish tectum. *Journal of Integrative Neuroscience*, 8, 323–344.
- Ewert, J. P. (1970). Neural mechanisms of prey-catching and avoidance behavior in the toad (Bufo bufo L.). Brain, Behavior and Evolution, 3, 36–56.
- Famiglietti, E. V. (2005a). Synaptic organization of complex ganglion cells in rabbit retina: Type and arrangement of inputs to directionally selective and local-edge-detector cells. *Journal of Comparative Neurology*, 484, 357–391
- Famiglietti, E. V. (2005b). "Small-tufted" ganglion cells and two visual systems for the detection of object motion in rabbit retina. *Visual Neuroscience*, 22, 509–534.
- Field, G. D., & Chichilnisky, E. J. (2007). Information processing in the primate retina: Circuitry and coding. *Annual Review of Neuroscience*, 30, 1–30.
- Gesteland, R. C., Howland, B., Lettvin, J. Y., & Pitts, W. H. (1959). Comments on microelectrodes. *Proceedings of the IRE*, 47, 1856–1862.
- Hubel, D. H., & Wiesel, T. N. (1968). Receptive fields and functional architecture of monkey striate cortex. *Journal of Physiology (London)*, 195, 215–243.
- Jacobson, M., & Gaze, R. M. (1964). Types of visual response from single units in the optic tectum and optic nerve of the goldfish. *Quarterly Journal of Experimental Physiology*, 49, 199–209.
- Kardamakis, A. A., Saitoh, K., & Grillner, S. (2015). Tectal microcircuit generating visual selection commands on gaze-controlling neurons. Proceedings of the National Academy of Sciences United States of America, 112, E1956–E1965.
- Kawasaki, M., & Aoki, K. (1983). Visual responses recorded from the optic tectum of the Japanese dace, *Tribolodon hakonensis*. *Journal of Comparative Physiology A*, 152, 147–153.
- Kim, I. J., Zhang, Y., Yamagata, M., Meister, M., & Sanes, J. R. (2008). Molecular identification of a retinal cell type that responds to upward motion. *Nature*, 452, 478–482.
- Lettvin, J. Y., Maturana, H. R., McCulloch, W. S., & Pitts, W. H. (1959). What the frog's eye tells to the frog's brain. *Proceedings of the IRE*, 47, 1940–1951.
- Levick, W. R. (1967). Receptive fields and trigger features of ganglion cells in the visual streak of the rabbits retina. *Journal of Physiology (London)*, 188, 285–307.
- Li, Y. N., Tsujimura, T., Kawamura, S., & Dowling, J. E. (2012). Bipolar cell Photoreceptor connectivity in zebrafish (*Danio rerio*) retina. *Journal of Comparative Neurology*, 520, 3786–3802.
- Liege, B., & Galand, G. (1971). Types of single-unit visual responses in the trout's optic tectum. In A. Gudikov (Ed.), Visual information processing and control of motor activity (pp. 63–65). Sofia: Bulgarian Academy of Sciences.
- Manteifel, Y. B., & Bastakov, V. A. (1989). Structure and function in the visual system of the frog. Fortcshritte der Zoology Progress, 35, 349–351.
- Marc, R. E. (1998). The structure of vertebrate retinas. In J. Toyoda (Ed.), The retinal basis of vision. Amsterdam: Elsevier.
- Masland, R. H. (2001). The fundamental plan of the retina. *Nature Neuroscience*, 4, 877–886.
- Masland, R. H. (2012). The neuronal organization of the retina. *Neuron*, 76, 266–280.
- Maximov, P. V., & Maximov, V. V. (2010). A hardware-software complex for electrophysiological studies of the fish visual system. Paper presented at

- the meeting of the International Symposium "Ivan Djaja's (Jaen Giaja) Belgrade School of Physiology", Belgrade, Serbia. Book of Abstracts: p. 151.
- Maximov, V. V. (2010). A model of receptive field of orientation-selective ganglion cells of the fish retina. *Sensornye Sistemy*, 24, 110–124 (in Russian).
- Maximov, V. V., Maximova, E. M., Damjanović, I., & Maximov, P. V. (2013). Detection and resolution of drifting gratings by motion detectors in the fish retina. *Journal of Integrative Neuroscience*, 12, 117–143.
- Maximov, V. V., Maximova, E. M., & Maximov, P. V. (2005a). Direction selectivity in the goldfish tectum revisited. Annals of the New York Academy of Sciences, 1048, 198–205.
- Maximov, V. V., Maximova, E. M., & Maximov, P. V. (2005b). Classification of direction selective units recorded in the goldfish tectum. Sensornye Sistemy, 19, 322–335 (in Russian).
- Maximov, V. V., Maximova, E. M., & Maximov, P. V. (2007). Colour properties of the direction-selective motion detectors projecting to the gold-fish tectum. Sensornye Sistemy, 21, 19–28 (in Russian).
- Maximova, E. M. (1969). Effect of intracellular polarization of horizontal cells on the activity of the ganglion cells in the fish retina. *Biophysica*, 14, 537–544.
- Maximova, E. M., Maximov, P. V., Damjanović, I., Aliper, A. T., & Zaichikova, A. A. (2018). Ganglion cells: local edge detectors (spot detectors) in rabbit, fish and frog retinas. Paper presented at the meeting of Symposium "Visionarium XVII", Tvarminne, University of Helsinki, Finland. Book of Abstracts.
- Maximova, E. M., & Maximov, V. V. (1981). Detectors of the oriented lines in the visual system of the fish Carassius carassius. Journal of Evolutionary Biochemistry and Physiology, 17, 519–525 (in Russian).
- Maximova, E. M., Orlov, O. Y., & Dimentman, A. M. (1971). Investigation of visual system of some marine fishes. *Voprocy Ichtiologii*, 11, 893–899 (in Russian).
- Maximova, E. M., Pushchin, I. I., Maximov, P. V., & Maximov, V. V. (2012). Presynaptic and postsynaptic single-unit responses in the goldfish tectum as revealed by a reversible synaptic transmission blocker. *Journal of Integrative Neuroscience*, 11, 183–191.
- Meek, J., & Schellart, N. A. M. (1978). A Golgi study of the goldfish optic tectum. *Journal of Comparative Neurology*, 182, 89–121.
- Mitarai, G. (1982). Chromatic properties of S-potentials in fish. In B. D. Drujan & M. Laufer (Eds.), *The S-potential* (pp. 137–150). New York: Liss.
- Nikolaou, N., Lowe, A. S., Walker, A. S., Abbas, F., Hunter, P. R., Thompson, I. D., & Meyer, M. P. (2012). Parametric functional maps of visual inputs to the tectum. *Neuron*, 76, 317–324.
- Northmore, D. P. M. (2011). The optic tectum. In A. P. Farrell (Ed.), *Encyclopedia of fish physiology: From genome to environment* (pp. 131–142). London, UK: Elsevier.
- O'Brien, B. J., Isayama, T., & Berson, D.M. (1999). Light responses of morphologically identified cat ganglion cells. *Investigative Ophthalmology & Visual Science*, 40, ARVO Abstract 815.
- Pigarev, I. N., & Zenkin, G. M. (1970). Dark spot detectors in the frog retina and their role in the organization of food behavior. *Zhurnal Vysshei Nervnoi Deiatelnosti Imeni I. P. Pavlova*, 20, 170 (in Russian).
- Preuss, S. J., Trivedi, C. A., vom Berg-Maurer, C. M., Ryu, S., & Bollmann, J. H. (2014). Classification of object size in retinotectal microcircuits. *Current Biology*, 24, 2376–2385.
- Robles, E., Filosa, A., & Baier, H. (2013). Precise lamination of retinal axons generates multiple parallel input pathways in the tectum. *Journal of Neuroscience*, 33, 5027–5039.
- Robles, E., Smith, S. J., & Baier, H. (2011). Characterization of genetically targeted neuron types in the zebrafish optic tectum. Frontiers in Neural Circuits, 5(Article 1), 1–14.
- Rodieck, R. W., & Watanabe, M. (1993). Survey of the morphology of macaque retinal ganglion cells that project to the pretectum, superior colliculus, and parvicellular laminae of the lateral geniculate nucleus. *Journal of Comparative Neurology*, 338, 289–303.
- Sridharan, D., Schwarz, J. S., & Knudsen, E. I. (2014). Selective attention in birds. *Current Biology*, 24, R510–R513.

- Stell, W. K., Kretz, R., & Lightfoot, D. O. (1982). Horizontal cell conectivity in goldfish. In B. D. Drujan & M. Laufer (Eds.), *The S-potential* (pp. 51–75). New York: Liss..
- Sümbül, U., Song, S., McCulloch, K., Becker, M., Lin, B., Sanes, J. R., ... Seung, H. S. (2014). A genetic and computational approach to structurally classify neuronal types. *Nature Communications*, *5*, 3512.
- Trivedi, C. A., & Bollmann, J. H. (2013). Visually driven chaining of elementary swim patterns into a goal-directed motor sequence: A virtual reality study of zebrafish prey capture. Frontiers in Neural Circuits, 7, 86.
- van Wyk, M., Taylor, W. R., & Vaney, D. I. (2006). Local edge detectors: A substrate for fine spatial vision at low temporal frequencies in rabbit retina. *Journal of Neuroscience*, 26, 13250–13263.
- Vaney, D. I. (1994). Territorial organization of direction-selective ganglion cells in rabbit retina. *Journal of Neurosciences*, 14, 6301–6316.
- Venkataramani, S., & Taylor, W. R. (2010). Orientation selectivity in rabbit retinal ganglion cells is mediated by presynaptic inhibition. *Journal of Neuroscience*, 30, 15664–15676.
- Vinogradova, V. M., Bastakov, V. A., Dyachkova, L. N., & Manteifel, Y. B. (1973). Restoration of retino-tectal connections in frogs during regeneration of the optic nerve. *Neirofiziologiya*, 5, 611–620 (in Russian).
- Volgyi, B., Chheda, S., & Bloomfield, S. A. (2009). Tracer coupling patterns of the ganglion cell subtypes in the mouse retina. *Journal of Compara*tive Neurology, 512, 664–687.
- Wartzok, D., & Marks, W. B. (1973). Directionally selective visual units recorded in optic tectum of the goldfish. *Journal of Neurophysiology*, 36, 588-604.

- Weng, S., Sun, W., & He, S. (2005). Identification of ON-OFF directionselective ganglion cells in the mouse retina. *Journal of Physiology* (*London*), 562, 915–923.
- Wingate, J. T., Fitzgibbon, T., & Thompson, I. D. (1992). Lucifer yellow, retrograde tracers, and fractal analysis characterise adult ferret retinal ganglion cells. *Journal of Comparative Neurology*, 323, 449–474.
- Zenkin, G. M., & Pigarev, I. N. (1969). Detector properties of the ganglion cells of the pike retina. *Biofizika*, 14, 722–730 (in Russian).
- Zhang, Y., Kim, I. J., Sanes, J. R., & Meister, M. (2012). The most numerous ganglion cell type of the mouse retina is a selective feature detector. Proceedings of the National Academy of Sciences United States of America, 109, E2391–E2398.
- Zhaoping, L. (2016). From the optic tectum to the primary visual cortex: Migration through evolution of the saliency map for exogenous attentional guidance. *Current Opinion in Neurobiology*, 40, 94–102.

How to cite this article: Maximova EM, Aliper AT, Damjanović I, Zaichikova AA, Maximov PV. On the organization of receptive fields of retinal spot detectors projecting to the fish tectum: Analogies with the local edge detectors in frogs and mammals. *J Comp Neurol*. 2019;1–13. https://doi.org/10.1002/cne.24824